

# Local and average behavior in inhomogeneous superdiffusive media

Alessandro Vezzani<sup>a,b,\*</sup>, Raffaella Burioni<sup>b,c</sup>, Luca Caniparoli<sup>d</sup> and Stefano Leprie<sup>e</sup>

<sup>a</sup>Centro S3, CNR-Istituto di Nanoscienze, Via Campi 213A, 41125 Modena Italy <sup>b</sup>Dipartimento di Fisica, Università degli Studi di Parma, viale G.P. Usberti 7/A, 43100 Parma, Italy; <sup>c</sup>INFN, Gruppo Collegato di Parma, viale G.P. Usberti 7/A, 43100 Parma, Italy; <sup>d</sup>International School for Advanced Studies SISSA, via Beirut 2/4, 34151, Trieste, Italy; <sup>e</sup>Istituto dei Sistemi Complessi, Consiglio Nazionale delle Ricerche, via Madonna del Piano 10, I-50019 Sesto Fiorentino, Italy

We consider a random walk on one-dimensional inhomogeneous graphs built from Cantor fractals. Our study is motivated by recent experiments that demonstrated superdiffusion of light in complex disordered materials, thereby termed Lévy glasses. We introduce a geometric parameter  $\alpha$  which plays a role analogous to the exponent characterizing the step length distribution in random systems. We study the large-time behavior of both local and average observables; for the latter case, we distinguish two different types of averages, respectively over the set of all initial sites and over the scattering sites only. The “single long jump approximation” is applied to analytically determine the different asymptotic behaviours as a function of  $\alpha$  and to understand their origin. We also discuss the possibility that the root of the mean square displacement and the characteristic length of the walker distribution may grow according to different power laws; this anomalous behaviour is typical of processes characterized by Lévy statistics and here, in particular, it is shown to influence average quantities.

PACS numbers:

## I. INTRODUCTION

The laws of Brownian motion crucially relies on the hypothesis that the steps for the diffusing particle are small (with finite variance) and uncorrelated. Whenever these assumptions are violated, the standard diffusion picture breaks down and anomalous phenomena emerge [1, 2].

In particular, transport processes where the step length distribution has a diverging variance have been theoretically studied in detail. Among those, one of the most interesting is the so-called Lévy walks [3, 4], in which particles perform independent steps  $l$  at constant velocity, with a distribution  $\lambda(l)$  following an algebraic tail  $\sim l^{-(1+\alpha)}$ . Such a distribution is said to be heavy-tailed and it is known to have a diverging variance for  $\alpha < 2$ . Since transport is thereby dominated by very long steps, the mean square displacement increases faster than linearly with time, hence the name superdiffusion.

Among the many possible experimental applications, our work is motivated by the recent realization of materials termed *Lévy glasses*, where light rays propagate through an assembly of transparent spheres embedded in a scattering medium [5, 6]. If the diameter of the spheres is power-law distributed, light can indeed perform anomalous diffusion. Owing to their ease of fabrication and tunability, such a novel material offers an unprecedented opportunity to study anomalous transport processes in a systematic and controllable way.

An important feature of the experimental samples is that the walk is correlated: light that has just crossed a large glass microsphere has a higher probability of being backscattered at the following step and thus to perform a jump of roughly the same length. While the case of

uncorrelated jumps is well understood [7], the correlation effects, that are expected to deeply influence the diffusion properties [8], are still to be characterized. To this aim, quenched Lévy processes have been studied on one dimensional systems [9, 10]. More recently, different aspects regarding the scaling properties of random-walk distributions, the relations between the dynamical exponents and the different average procedures have been discussed in a common framework [11].

In order to get a deeper insight on the effect of step-length correlations, a class of deterministic, one-dimensional models called *Cantor graphs* has been introduced [12]. Random walks on these structures perform correlated long jumps induced by the underlying fractal topology. As the latter is generated by deterministic rules, diffusion properties can be studied in a simpler way than in the random case. Here we extended to this deterministic topologies some of the results proved in [11] for random structures. In particular, we introduce a geometric parameter  $\alpha$  which plays the same role as the exponent characterizing the step length distribution  $\lambda(l)$  in random systems. Three kinds of statistical averaging are introduced: (i) a local one, namely the average of all trajectories starting from a given initial site (whose asymptotic behaviour being expected to be independent of the site choice); (ii) an averaging over *all* possible initial sites of the graph and (iii) averages where *only* scattering sites are considered as initial conditions. In the random case, the differences between such averaging procedures have been evidenced in [9, 11]. On deterministic structures, average procedures (i) and (ii) have been discussed in [12]. Here we complete the picture studying the effect of averaging over scattering sites. We evidence that the behavior of the mean square displacement is similar

to random case; while the probability density displays a more complex structure being given by a non-trivial time-dependent superposition of step functions. We remark that, in experiments [5, 6], light enters the sample with a scattering event and averages of type (iii) are the most physically sensible quantities to compare with. Interestingly, in Lévy processes the root of the mean square displacement and the characteristic length of the distributions may grow according to different power laws; here, in particular, this strongly anomalous behavior characterizes average quantities.

The paper is organized as follows. In the next section we introduce the directed Cantor graphs and we define a simple random walk on these structures. We then discuss the relevant physical quantities and the average procedures. Section 4 is devoted to discuss the scaling hypothesis and the single long jump approximation, which allows to evaluate the tails of the density distribution. Finally, in Section 5 we discuss our results evidencing differences among averaging procedures. In particular for the case (i) and (ii) we review the results presented in [12] presenting new numerical data, while for the case of average over scattering sites, which has not been discussed so far for the deterministic structures, we provide a sketch of the derivation of the dynamical exponents within the single long jump approximation and we compare the result with numerical simulations. In general the new simulations evidence that the probability density presents different asymptotic behaviors depending on the average procedures, clearly supporting both the scaling hypothesis and the single long jump approach. Moreover the asymptotic behavior of the mean square displacement have been tested for a wider range of  $\alpha$ 's.

## II. RANDOM WALKS ON CANTOR GRAPHS

In paper [12] we have introduced a class of graphs, denoted as directed Cantor graphs, as a one-dimensional, deterministic counterpart of the geometric structure of the Lévy glass materials mentioned above [5]. Indeed, random walks on the Cantor graphs display a superdiffusive Lévy like motion analogous to the the one of light in such inhomogeneous glassy material.

The class of graphs we will consider is defined by two parameters, denoted as  $n_r$  and  $n_u$ , and describing the growth of the fractal from generation  $G-1$  to generation  $G$ . In particular the fractal  $\mathcal{G}$  of generation  $G$  is built connecting  $n_r$  fractals of generation  $G-1$  by  $n_r-1$  unidirectional bubbles of length  $L_G = n_u^{G-1}$ , as shown in Figures 1 and 2.

A simple random walk [13] is naturally defined on these structures: undirected links connect sites in both directions while directed links have to be crossed only in the prescribed way. A site is called *bidirectional* if the walker placed on that site can move in both directions (and the two possible moves are performed with probability 1/2). A site is instead called *unidirectional* if the walker is al-

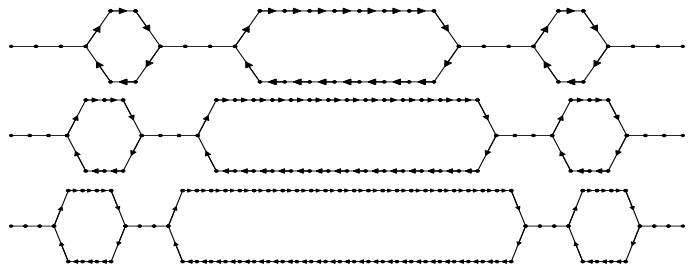


FIG. 1: The generation  $G = 3$  of the graph with  $n_u = 3, 4, 5$ , in the  $n_r = 2$  case.

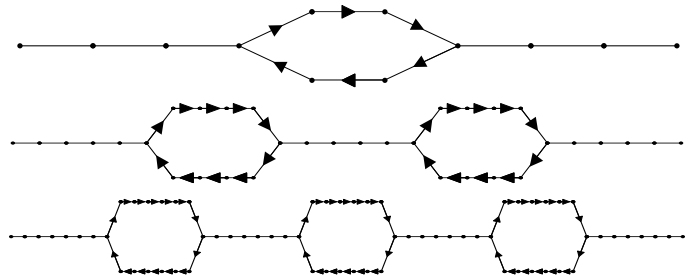


FIG. 2: Three examples of Cantor graphs of generation  $G = 2$  with  $n_r = 2, 3, 4$  and  $n_u = 3, 4, 5$ .

lowed to move only in one direction (in this case the move is performed with probability one, i.e. ballistic motion). All the links have unitary length and are crossed at constant velocity  $v$ . The number of bidirectional sites  $N_b$  and unidirectional sites  $N_u$  present at generation  $G$  is given by:

$$N_b = 2n_r^G, \quad N_u = \frac{(n_u - 1)n_r^G - (n_r - 1)n_u^G}{n_r - n_u} + 1 \quad (1)$$

where we use the convention of counting only once the couple of sites of the bubbles at the same distance from the origin. The total number of sites at generation  $G$  is hence  $N_G = N_b + N_u$ . In the following, an important parameter for the description of the structure will be the ratio  $\alpha = \log(n_r)/\log(n_u)$ . For  $\alpha < 1$ , the graphs are called *slim*, as the fraction of bidirectional sites vanishes in the thermodynamic limit, i.e.  $\lim_{G \rightarrow \infty} N_b/N_G = 0$ . On the contrary, for  $\alpha > 1$  graphs are called *fat*, since a finite fraction of bidirectional sites is present, and  $\lim_{G \rightarrow \infty} N_b/N_G > 0$ .

## III. PHYSICAL QUANTITIES AND AVERAGES

Let  $P_i(r, t)$  be the probability of arriving at distance  $r$  starting from  $i$  in  $t$  steps. In general,  $P_i(r, t)$  depends on the starting site  $i$ . However for large enough space scales (i.e.  $r$  much larger than the distance between  $i$  and an origin  $i = 1$ ) the asymptotic properties of  $P_i(r, t)$  are expected to be site independent and hence to describe a

property of the whole graph, i.e.  $P_i(r, t) \sim P_1(r, t)$ . In particular, the asymptotic behaviour of the mean square displacement

$$\langle r_i^2(t) \rangle = \int_0^{vt} P_i(r, t) r^2 dr \quad (2)$$

should be independent of  $i$ . The integration cutoff in (2) is provided by the fact that the walker covers at most a distance  $vt$  in a time  $t$  ( $v = 1$  in the following). Another important quantity whose asymptotic behaviour depends only on the large scale topology of the structure is the resistivity  $R_i(r)$  i.e the number of bidirectional sites whose distance from  $i$  is smaller than  $r$ .

On inhomogeneous structures, average and local properties are in general different [14], and in structures characterized by long tails, different averaging procedures can yield different results as well [9, 11]. In particular, on Cantor graphs one can distinguish between the average over all starting sites, i.e.:

$$\bar{P}(r, t) = \lim_{G \rightarrow \infty} \frac{\sum_{i \in \mathcal{G}} P_i(r, t)}{N_G} \quad (3)$$

and the averages on processes beginning with a scattering event:

$$\tilde{P}(r, t) = \lim_{G \rightarrow \infty} \frac{\sum_{i \in \mathcal{G}_b} P_i(r, t)}{N_b} \quad (4)$$

where  $\mathcal{G}_b$  is the set of the bidirectional sites belonging to graphs of generation  $G$ . The same averaging procedures can be introduced also for different quantities. One can consider the average resistivity  $\bar{R}(r)$  and  $\tilde{R}(r)$  and, as in (2), one can also define the average mean square distances  $\langle \bar{r}^2(t) \rangle$  and  $\langle \tilde{r}^2(t) \rangle$ .

Since the resistivity can be evaluated by simply counting the number of sites in a given generation, one obtain the following asymptotic behaviours:

$$R_1(r) \sim \tilde{R}(r) \sim \begin{cases} r^\alpha, & \text{if } \alpha < 1 \\ r & \text{if } \alpha \geq 1 \end{cases} \quad (5)$$

$$\bar{R}(r) \sim \begin{cases} 0 & \text{if } \alpha < 1 \\ r & \text{if } \alpha \geq 1. \end{cases} \quad (6)$$

These results represent the deterministic analog of the expressions for the resistivity obtained in a random sample in [10].

#### IV. THE SCALING HYPOTHESIS AND THE SINGLE LONG JUMP APPROXIMATION

The most general scaling hypothesis for the probabilities  $P_1(r, t)$  is:

$$P_1(r, t) = \ell_1^{-1}(t) f_1(r/\ell_1(t)) + g_1(r, t) \quad (7)$$

with a convergence in probability

$$\lim_{t \rightarrow \infty} \int_0^t |P_1(r, t) - \ell_1^{-1}(t) f_1(r/\ell_1(t))| dr = 0 \quad (8)$$

The leading contribution to  $P_1(r, t)$  is hence  $\ell_1^{-1}(t) f_1(r/\ell_1(t))$  which is significantly different from zero only for  $r \lesssim \ell_1(t)$ . The subleading term  $g_1(r, t)$ , with  $\lim_{t \rightarrow \infty} \int |g_1(r, t)| dr = 0$  describes the behavior at larger distances, i.e.  $\ell_1(t) \ll r < t$ . Notice that, if  $g_1(r, t)$  does not vanish rapidly enough, it can nevertheless provide important contributions to  $\langle r_1^2(t) \rangle$ . The same scaling ansatz should be valid also for the average probabilities  $\bar{P}(r, t)$  and  $\tilde{P}(r, t)$  by introducing suitable averaged scaling length and scaling functions  $\bar{f}(r/\bar{\ell})$ ,  $\tilde{f}(r/\tilde{\ell})$ , and suitable averaged long distance corrections  $\bar{g}(r, t)$ ,  $\tilde{g}(r, t)$ .

In [12, 15] it has been proved that the growth of the characteristic length can be directly related to the growth of the resistance. We define the exponent describing the growth of the correlation length as:

$$\ell_1(t) \sim t^{d_s/2}. \quad (9)$$

so that in analogy with standard definition of random walks [16], we get  $P_1(0, t) \sim t^{-d_s/2}$ . Then using the scaling relations proved in [12, 15] we obtain

$$R_1(r) \sim r^{2/d_s-1}. \quad (10)$$

Analogous relations hold for the average quantities, in terms of the average scaling lengths. Introducing the known results for the resistivity (5,6), one obtains the following behaviors for the scaling lengths:

$$\ell_1(t) \sim \tilde{\ell}(t) \sim \begin{cases} t^{\frac{1}{1+\alpha}}, & \text{if } \alpha < 1 \\ t^{\frac{1}{2}} & \text{if } \alpha \geq 1 \end{cases} \quad (11)$$

$$\bar{\ell}(t) \sim \begin{cases} t & \text{if } \alpha < 1 \\ t^{\frac{1}{2}} & \text{if } \alpha \geq 1 \end{cases} \quad (12)$$

Let us now discuss the behaviour of the mean square displacements. When only lengths of order  $r \lesssim \ell(t)$  provide significant contributions to the integral (2), the standard relation  $\langle r^2(t) \rangle \sim \ell^2(t)$  holds and the asymptotic behaviour coincides with those given by (11,12). However it is known that, in presence of long tailed distributions, anomalies with respect to this behaviour can be present. In particular it has been evidenced in [9, 11] that a key role is played by long jumps, leading the walker to a distance  $r \gg \ell(t)$ . In the random case, consideration of a single long jump actually accounts for the asymptotic behaviour [11]. Indeed, these processes can give rise to two different types of corrections to  $P(r, t)$ . First, they can produce a zero-measure function  $g(r, t)$ , providing a significant contribution to  $\langle r^2(t) \rangle$ ; second, the scaling

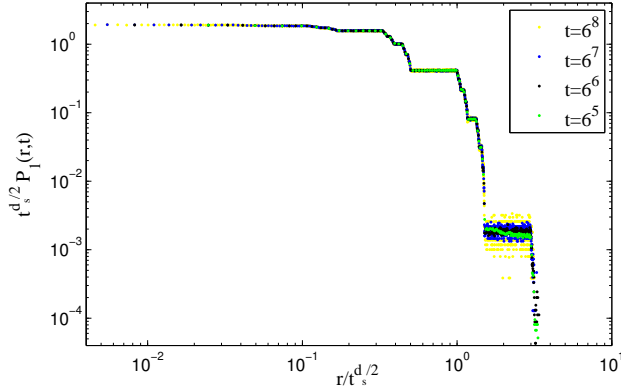


FIG. 3: Dynamical scaling of the probability for initial site  $i = 1$  on the graph obtained with  $n_r = 2$  and  $n_u = 3$ . Note the fast decay of the scaling function. The stepwise structure of the scaling function is due to the fractality of the graph.

function  $f(x)$  can feature a long tail, breaking the proportionality between  $\langle r^2(t) \rangle$  and  $\ell^2(t)$ . Here we will evidence that these anomalies, originating from the single long jump, are also present in the deterministic graphs and they are deeply influenced by the averaging procedures.

## V. RESULTS

### A. Local behaviour

Let us first consider the local properties. In this situation we can focus on processes starting from the origin  $i = 1$  of the graph. Indeed, if  $r$  is much larger than the distance between  $i$  and 1, we expect that  $P_i(r, t)$  should behave as  $P_1(r, t)$  and hence the asymptotic behaviour should be the same for any starting point. When starting from the origin, in a time  $t$  the walker typically covers a distance  $\ell_1(t)$  and, in the deterministic graphs, within such distance there are no bubbles of length larger than  $\ell_1(t)$ . Therefore, long jumps do not occur and  $\langle r_1^2(t) \rangle \sim \ell_1^2(t)$ . Therefore [12]

$$\langle r_1^2(t) \rangle \sim \begin{cases} t^{\frac{2}{1+\alpha}}, & \text{if } \alpha < 1 \\ t & \text{if } \alpha \geq 1 \end{cases} \quad (13)$$

Figure 3 reports, an example the probability density  $P_1(r, t)$  obtained by a Montecarlo simulation. The data provide a clear evidence that the scaling function presents a fast decay confirming our hypothesis of no long jump. As explained in [12] the fractal structure give rise to log-periodic oscillations which can be discarded considering peculiar sequence of times (in this case  $t = 6^k$ ), However, such oscillations do not change the general framework of the scaling hypothesis. The growth of  $\langle r_1^2(t) \rangle$  is plotted

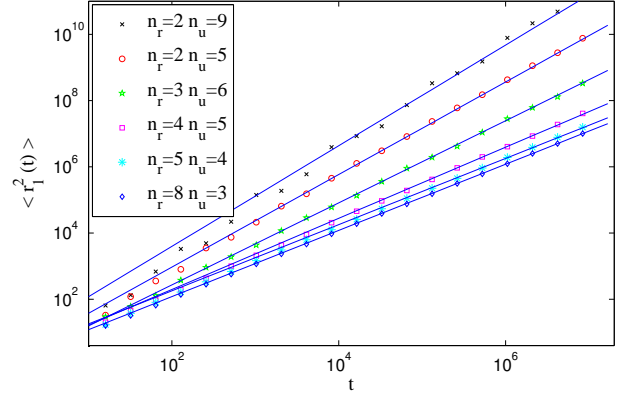


FIG. 4: Growth of the mean square displacements for initial site  $i = 1$ . Power-law fits give exponents in very good agreement with the theoretical values, in equation (13).

in Figure 4, the continuous lines represent the expected behaviors (13).

### B. Averages over all sites

When averaging over all the sites, it has been evidenced [12] that for  $\alpha < 1$  the motion is always ballistic, while for  $\alpha > 1$  the situation is much more complex, since the walker can perform a single jump much larger than  $\ell(t)$ . Typically, such a long jump occurs at the first step because, with a random choice of the starting point, the probability of belonging to a large bubble is much larger at  $t = 0$  than during the rest of the evolution. In this situation, one can estimate the zero measure correction to  $\bar{P}(r, t)$  obtaining  $\bar{g}(r, t) \sim t^{-\alpha+1} \delta(r - t)$ , i.e. a peak associated with the ballistic motion of the particle, weighted by a factor  $t^{-\alpha+1}$  representing the probability of belonging to a bubble larger than  $t$  at the initial time. The behavior of  $P(r, t)$  is illustrated in the simulations of figure 5 evidencing the presence of a scaling regime for  $r \lesssim \ell(t)$  and of ballistic peaks at large  $r$  whose height evolves as  $t^{-\alpha+1}$  (dashed line). Even if  $\bar{g}(r, t)$  provides a subleading contribution to  $\bar{P}(r, t)$ , the integral in (2) is dominated by  $\bar{g}(r, t)$  for  $1 < \alpha < 2$  and by  $\bar{f}(r/\ell(t))$  only when  $\alpha > 2$ . Therefore the behaviour of the mean square displacement is

$$\langle \bar{r}^2(t) \rangle \sim \begin{cases} t^{3-\alpha}, & \text{if } 1 < \alpha < 2 \\ t & \text{if } \alpha \geq 2 \end{cases} \quad (14)$$

while the motion is purely ballistic for  $\alpha < 1$ . Figure 6 shows that the predicted exponents (14) are well verified.

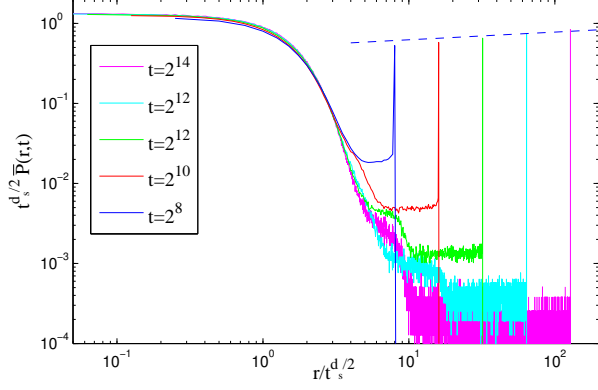


FIG. 5: Dynamical scaling of  $\bar{P}(r, t)$  in the average case. The data refer to the case  $n_r = 7$   $n_u = 4$ . Ballistic peaks at  $r = t$  scale as  $t^{1-\alpha}$  (dashed line), while for  $r \lesssim \tilde{\ell}(t)$  the scaling hypothesis is well satisfied.

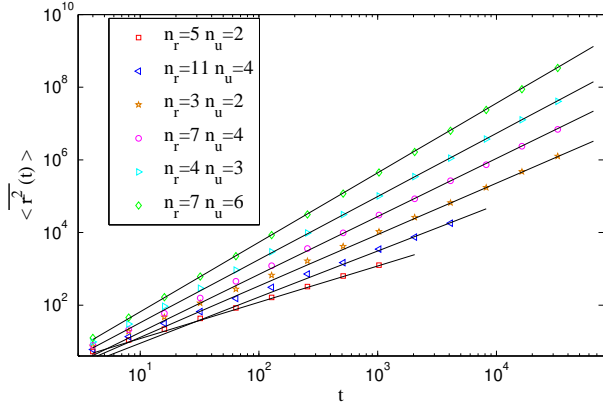


FIG. 6: Growth of the mean square displacements when average over scattering over the whole sample is considered. We compare the numerical results with the theoretical predictions (14) in both the regimes  $1 < \alpha < 2$  and  $\alpha > 2$ .

### C. Averages over bidirectional sites

In [11] it has been shown that, for random systems, averages over bidirectional scattering sites can provide different results with respect to averages over all starting points and a scaling approach has been discussed, based on the single long jump approximation. Here we introduce an analogous argument for the deterministic graph.

In the case of average over bidirectional sites, the single long jump does not occur necessarily at the first step. In particular for the deterministic graph the probability of performing a jump of length  $L_k = n_u^k \gg \tilde{\ell}(t)$  in a time  $t$  is  $N(t)n_r^{-k}$  where  $N(t)$  is the number of bidirectional sites visited by the walker in a time  $t$  and  $n_r^{-k}$  is the probability that a bidirectional site belongs to a bubble of length  $L_k$ .

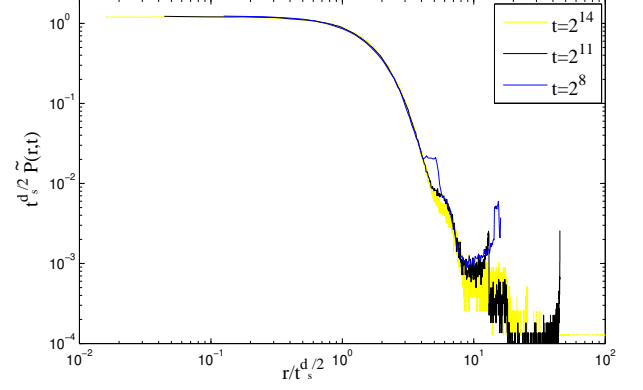


FIG. 7: The dynamical scaling of  $\tilde{P}(r, t)$  in the case of averages over bidirectional sites. Here we plot the case  $n_r = 4$  and  $n_u = 3$ . For  $r \lesssim \tilde{\ell}(t)$  the scaling hypothesis (7) is very well verified with  $\tilde{\ell}(t)$  growing as indicate in (11). For larger  $r$  the behaviour is much more complicated since the tails are composed by a superpositions of step functions.

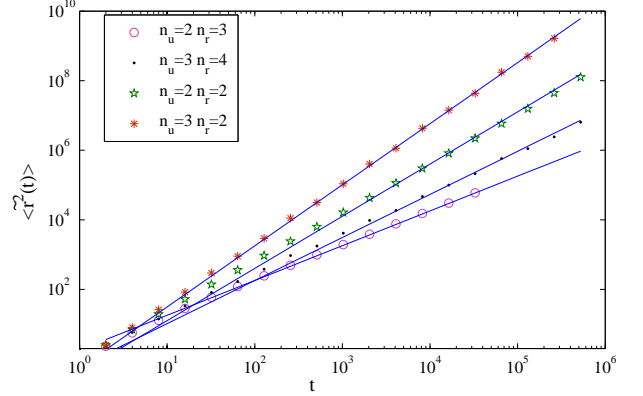


FIG. 8: Growth of the mean square displacement when averaged over bidirectional sites is considered. The results are compared with the theoretical predictions (18) given by the continuous lines. Different values of  $n_r$  and  $n_u$  are considered, showing that the predictions (18) are verified in the different regimes of  $\alpha$ 's.

Discarding this long jump, the distance crossed by the walker in a time  $t$  is of order  $\tilde{\ell}(t)$ , and therefore, according to the behaviour of the resistivity described by equations 5,  $N(t) \sim \tilde{\ell}(t)^\alpha$  for  $\alpha < 1$  and  $N(t) \sim \tilde{\ell}(t)$  for  $\alpha \geq 1$ . The main difference with respect to the random case is that now the only possible lengths of the long jumps are given by the sizes  $L_k$  of the bubbles in the fractal. Hence, for  $\tilde{\ell}(t) < r < t$ ,  $\tilde{P}(r, t)$  is a complex step function where both integers  $n_u$  and  $n_r$  plays a non trivial role. However, the contribution to the mean square displacement can be

evaluated as follows:

$$N(t) \left( \sum_{\tilde{\ell}(t) < L_k < t} \frac{n_u^{2k}}{n_r^k} + t^2 \sum_{L_k > t} \frac{1}{n_r^k} \right) \quad (15)$$

where the first sum is related to the bubbles of length  $L_k$  ( $\tilde{\ell}(t) < L_k < t$ ) providing a contribution to the mean square displacements of order  $L_k^2 = n_u^{2k}$ , while the second sum comes from the bubbles of length larger than  $t$ , providing a contribution  $t^2$ . Expanding equation 15 for large times one obtains the asymptotic behaviours

$$N(t) \left( \sum_{\tilde{\ell}(t) < L_k < t} \frac{n_u^{2k}}{n_r^k} + t^2 \sum_{L_k > t} \frac{1}{n_r^k} \right) \sim t^{\frac{2+2\alpha+\alpha^2}{1+\alpha}} \quad (16)$$

for  $\alpha < 1$  and

$$N(t) \left( \sum_{\tilde{\ell}(t) < L_k < t} \frac{n_u^{2k}}{n_r^k} + t^2 \sum_{L_k > t} \frac{1}{n_r^k} \right) \sim t^{5/2-\alpha} \quad (17)$$

for  $\alpha > 1$ . The first expression is always dominant with respect  $\tilde{\ell}(t)$ , while the second expression becomes sub-leading for  $\alpha > 3/2$ . The overall behaviour of the mean square displacement is summarized as follows:

$$\langle \tilde{r}^2(t) \rangle \sim \begin{cases} t^{\frac{2+2\alpha+\alpha^2}{1+\alpha}} & \text{if } 0 < \alpha < 1 \\ t^{\frac{5}{2}-\alpha} & \text{if } 1 \leq \alpha \leq 3/2 \\ t & \text{if } 3/2 < \alpha \end{cases} \quad (18)$$

Equations (18) extend the results of the random case to the deterministic topology described by the directed Cantor graphs. Clearly the complex shape of the scaling function (15) determines the presence of logperiodic oscillations superimposed to (18), which is a typical behaviour of fractal structures [17]. Figure (7) evidences that the dynamical scaling is well verified for  $r \lesssim \tilde{\ell}(t)$ , while at larger distances  $\tilde{P}(r, t)$  is characterized by a superposition of slowly decaying step functions as predicted by (15). Figure (8) evidences by means of Montecarlo simulations that Equations (18) are well verified for large times in the whole range of  $\alpha$ 's.

### Acknowledgements

We acknowledge useful discussion with P. Barthelemy, J. Bertolotti, R. Livi, D.S. Wiersma, K. Vynck. This work is partially supported by the MIUR project PRIN 2008 *Non linearity and disorder in classical and quantum processes*.

- 
- [1] J.P. Bouchaud and A. Georges, Phys. Rep. 195 (1990) p. 127; D. ben-Avraham and S. Havlin, *Diffusion and Reactions in Fractals and Disordered Systems*, Cambridge University Press, 2004
  - [2] R.Klages, G. Radons and I.M. Sokolov (Eds.) *Anomalous Transport: Foundations and Applications* (Wiley, VCH Berlin), 2008.
  - [3] A. Blumen, G. Zumofen, and J. Klafter, Phys. Rev. A **40**, 3964 (1989).
  - [4] J. Klafter, A. Blumen, G. Zumofen, and M. F. Shlesinger, Physica A, **168** 637 (1990).
  - [5] P. Barthelemy, J. Bertolotti and D.S. Wiersma, Nature 453 495 (2008).
  - [6] J. Bertolotti, K. Vynck, L. Pattelli, P. Barthelemy, S. Lepri, D.S. Wiersma Adv. Funct. Mat. 20 Issue 6 , 965 - 968 (2010)
  - [7] T. Geisel, J. Nierwetberg and A. Zacherl Phys. Rev. Lett. 54 616 (1985), M. F. Shlesinger, G. M. Zaslavski and J. Klafter Nature, 363 31 (1993), G. Zumofen and J. Klafter Phys. Rev. E 47, 851 (1993).
  - [8] H.C. Fogedby, Phys. Rev. Lett. 73 2517 (1994), R. Kutner and P. Maass, J. Phys. A: Math. Gen. 31, 2603 (1998), M. Schulz, Phys. Lett. A , 298, 105 (2002).
  - [9] E. Barkai, V. Fleurov, J. Klafter, Phys. Rev. E 61 1164 (2000).
  - [10] C.W.J. Beenakker, C.W. Groth, A.R. Akhmerov, Phys. Rev. B 79, 024204 (2009).
  - [11] R. Burioni, L. Caniparoli, S. and A. Vezzani Phys. Rev. E 81, 060101 (2010)
  - [12] R. Burioni, L. Caniparoli, S. Lepri and A. Vezzani Phys. Rev. E 81, 011127 (2010).
  - [13] E. W. Montroll and G. H. Weiss, J. Math. Phys. 6 (1965) p. 167.
  - [14] R. Burioni and D. Cassi, J. Phys. A 38, R45-R78 (2005).
  - [15] M.E. Cates, J. Physique 46, (1985) p.1059.
  - [16] S. Alexander and R. Orbach, J. Physique Lett. 43 (1982) p. L62.
  - [17] P.J. Grabner and W. Woess, Stoc. Proc. Applic. 69, (1997) p. 127.